J. Water Environ. Nanotechnol., 5(2): 147-156 Spring 2020

ORIGINAL RESEARCH PAPER

Removal of 2,4-dichlorophenoxyacetic acid from aqueous solutions by modified magnetic nanoparticles with amino functional groups

Reza Jazini Zadeh, Mohammad Hossein Sayadi *, Mohammad Reza Rezaei

Department of Environmental Engineering, Faculty of Natural Resources and Environment, University of Birjand, Birjand, Iran

Received: 2020-03-16 Accepted: 2020-04-21 Published: 2020-05-01

ABSTRACT

The present study was performed on the adsorption of 2,4-Dichlorophenoxyacetic acid from aqueous solutions by amine-modified magnetic nanoparticles. The adsorbent was synthesized by the co-precipitation method. The adsorbent properties of Fe_3O_4@SiO_2-NH_2 were investigated using XRD, FTIR, TGA, VSM, and TEM. Adsorbent efficacy was studied by investigating the effect of pH, initial concentration of pollutants, and adsorbent dose, and times. Finally, kinetics equations and isotherms models were used to describe the data. The results showed that the highest removal percentage was observed at pH 6 and the initial concentration of 20 mg/l of 2,4-Dichlorophenoxyacetic acid. The adsorption capacity was increased by 65.3% bypassing the time from the beginning of the process to 60 min. The results from the study of isotherms and adsorption kinetics presented that the sorption procedure follows the pseudo-second-order kinetics and the Langmuir isotherm with R2> 99. The maximum adsorption capacity of Fe_3O_4@SiO_2-NH_2 is 116.3 mg/g. Besides, thermodynamic studies have shown that the adsorption process in the present study is endothermic and spontaneous. The experiments showed that Fe_3O_4@SiO_2-NH_2 synthesized nanoparticles could be an excellent method to remove 2,4- Dichlorophenoxyacetic acid contaminants from the aqueous solutions due to the high efficiency, simplicity, and lack of secondary contamination in the solution.

Keywords: *adsorption, herbicides, isotherm, kinetics, water pollution*

How to cite this article

Jazini Zadeh R., Sayadi MH., Rezaei MR. Removal of 2,4-dichlorophenoxyacetic acid from aqueous solutions by modified magnetic nanoparticles with amino functional groups. J. Water Environ. Nanotechnol., 2020; 5(2): 147-156.

DOI: 10.22090/jwent.2020.02.005

INTRODUCTION

Today, agricultural pesticides are considered as one of the most serious environmental problems in the world. Pesticides can enter surface water and groundwater through the surface runoff, wind aerosols, leaching from soil and plant surfaces, discharge of agricultural and industrial wastewater [1,2]. 2,4-Dichlorophenoxyacetic acid (2,4-D) is one of the oldest herbicides selected from the phenoxy acetic acid group. 2,4-D is often used to remove broadleaf weeds such as sugarcane, wheat, rice, corn, cocoa, rubber and recreational areas, horticulture, golf courses, and pastures [3]. 2,4-D can inactivate the indoleacetic oxidase when consuming in the plant and increase the concentration of toxin in plant tissues, ultimately disrupt the plant growth and plant death [4]. Giving to the World Health Organization (WHO), the herbicides are classified as a class II toxin that can cause diseases such as neurotoxicity, hepatic toxicity, immunotoxicity, teratogenicity, an endocrine disorder, renal toxicity, and the production of epithelial cell in the human body [5, 6]. The resistance of 2,4-D is high in the environment and it is not easily chemically degraded compared to other herbicides [7]. 2,4-D can easily enter water sources after using due to its polarity and relatively good solubility in water and cause contamination of water and soil [8]. According to the WHO, the maximum permitted dose of 2,4-

* Corresponding Author Email: *mh_sayadi@birjand.ac.ir*

D in drinking water is 0.03 mg/l [9]. Given that, the conventional treatment processes of drinking water, including coagulation, sedimentation, filtration, and disinfection, can remove a small and polar molecule hardly. As a result, the use of more effective methods is unavoidable [10]. Various ways have been considered to remove 2,4-D toxin from aqueous sources, including advanced oxidation processes (Fenton, photo-Fenton, UV/H_2O_2, UV/TiO_2), ion exchange, ozonation, electrochemical, adsorption, photocatalytic, biological and photochemical [3]. Among these methods, surface adsorption is used due to the advantages such as the removal of organic and mineral materials at low concentrations, process simplicity, lack of sludge and mineral formation at low levels, adsorbent regeneration, and low cost of investment [11]. Recently, many adsorbents such as active carbon, iron oxide, compost, manganese oxide, clays, resin, and coal gray have been used to absorb heavy metals and some organic compounds from aquatic environments. Some adsorbents have a low surface-to-mass ratio which reduces the efficiency of adsorption process [12]. In recent years, nanomaterials have been used in aqueous solutions to remove toxins due to properties such as high surface-to-mass ratios, and high reactivity. In the meantime, iron nanoparticles are more widely used due to their availability, cheapness, non-toxicity, rapid reaction and high capacity [13]. Since the use of pure magnetite nanoparticles causes more tendency and accumulation of magnetic nanoparticles to each other and their instability in acidic solutions, it can cover them with various mineral coatings. Meanwhile, silica coating is one of the effective options that can improve the stability of nanoparticles in suspension, create more bonding of nanoparticles with organic ligands and prevent oxidation against air or oxygen [14,15]. Silica-coating magnetic nanoparticles and functionalized with active groups such as thiol, amino, and carboxyl have been developed [14]. The magnetite Fe_3O_4 nanoparticles are synthesized and amino-functionalized Fe_3O_4@SiO_2-NH_2 magnetic nanoparticles [16]. The Fe_3O_4@SiO_2 was synthesized by silica source that extracted from rice husk. Afterward, functionalized by 3-aminopropyltrimethoxysilane via post-synthesis grafting for selectivity improvement of methyl red color adsorption [17]. So given that few studies have been conducted on the removal of herbicides from the aquatic environment, this research aimed to synthesis of Fe_3O_4 magnetic then cover by SiO_2 and finally functionalized by -NH_2. After that the adsorption of 2,4-D from aqueous solutions by Fe_3O_4@SiO_2-NH_2 nanoparticles were studied.

MATERIALS AND METHODS

Materials (chemical and reagent)

The materials used in this study included Ferric chloride hexahydrate ($FeCl_3.6H_2O$; (as Iron (III)) and Ferric chloride tetrahydrate ($FeCl_2.4H_2O$; as Iron (II)), tetraethyl orthosilicate (TEOS), (3-Aminopropyl)trimethoxysilane (APTMS), herbicide 2,4-dichlorophenoxyacetic acid 95 %, HNO_3 (0.1M) and NaOH (0.1M) ammonia 25%, toluene, and ethanol (all Merck company).

Synthesis of Fe_3O_4@SiO_2-NH_2 nanoparticles

The Fe_3O_4@SiO_2-NH_2 nanoparticles were synthesized in the following three stages:

The first stage of synthesis of Fe_3O_4 magnetic nanoparticles

The chemical coprecipitation method was selected for the synthesis of Fe_3O_4 magnetic nanoparticles. For this purpose, 22 g of $FeCl_3.6H_2O$ and 8 g of $FeCl_2.4H_2O$ were mixed with 400 ml of deionized water in a beaker and then transferred to a reactor. Meanwhile, the reactor temperature was set at 80°C and stirred severely for 1 hour in the presence of nitrogen gas (600 rpm). Finally, by adding a certain amount of ammonia (25%) to the mixture, the solution color was changed to brown or black [3, 17].

The second stage of the synthesis of Fe_3O_4@SiO_2 nanoparticles

In this stage, 15 ml of tetraethyl orthosilicate solution with some ethanol was injected into the reactor as drop by drop to cover by SiO_2. Then it was stirred for 2 h at 90°C in the presence of nitrogen gas. After cooling to room temperature, the obtained suspension was washed several times with distilled water and Fe_3O_4 @SiO_2 nanoparticles were produced [14].

The third stage of modification of Fe_3O_4@SiO_2-NH_2 magnetic silica nanoparticle

In this step, 3g of nanoparticle of the previous stage with a 1to1 ratio of toluene and methanol solution (300 ml of each) was mixed with 10 ml of APTMS and heated at 30 to 80°C. At this stage, the reaction time increases with increasing temperature

Table 1. The values of the absorption kinetic parameters of the 2,4-D solution on Fe_3O_4@SiO_2-NH_2

order model	Expression	q_e	K_1,K_2	R^2
Pseudo-first-order model	$In(q_e-q_t)=Inq_e-K_1t$	99.009	0.00105	0.8935
Pseudo-second-order model	$t/q_e=1/K_2q_e^2+t/q_e$	71.928	0.00075	0.9936

(80°C). This causes more toluene to be released and destroys the hydrogen bonds, increasing the density of the amine functional group on the nanoparticle. This issue was done for 24 hours. Finally, the Fe_3O_4@SiO_2-NH_2 was washed several times with ethanol and deionized water, then dried at 80°C [16, 18].

The instrument for characterization of synthesized Fe_3O_4@SiO_2-NH_2

X-ray diffractometer with Philips X'pert device was used to investigate the structure of synthesized nanoparticles. The successful conjugation of SiO_2 and NH_2 onto the surface of the Fe_3O_4 nanoparticles was confirmed by FT–IR spectroscopy using BRUKER VECTOR 22 device in the range of 400 to 4000cm^{-1} using KBr tablet method. The Thermographic Analysis (TGA) was performed using the Perkin Elmer device (USA) at 50 to 1000°C. Transmission Electron Microscopy (TEM; Hitachi, Japan) techniques were used to identify the morphological structure of nanoparticles. To investigate the magnetic properties of the synthesized nanoparticles, a VSM analysis taken with the Daneshpajouh MDKB model was used in the magnetic range of -9000 to Oe 9000.

Batch sorption experiments

In this study, the effect of changing each of the parameters on the adsorption rate with the stability of other parameters was investigated. All adsorption tests were performed in a 100cc beaker with variable values of adsorbent dose, initial concentration of 2,4-D, and pH at 5 to 120 min. First, the pH of the tested samples was adjusted using nitric acid (0.1M) and sodium hydroxide (0.1M) in the range of 3 to 11. After determining the optimal pH, the samples with different concentrations of 5–50 mg/l of herbicide 2,4-D and then the adsorbent dose (0.1, 0.2, 0.3, 0.4, and 0.5g/l were tested. Finally, after (5, 15, 30, 60, 90, and 120 min), the concentrations before and after the adsorption of herbicide using a by spectrophotometer Bio spec-1601 were analyzed. The adsorbent was separated from the solution by a magnet.

Adsorption calculations and modeling

All adsorption tests have been performed to determine the kinetics, isotherms, and thermodynamics in the optimal values obtained. Equations 1 calculated the removal percentages of 2,4-D.

$$\%R=[(C_i-C_e)/ C_i] \times 100 \quad (1)$$

Here %R is the removal percentages of 2,4-D, $C_{i,}$ and C_e is the initial concentration and the equilibrium concentration in mg/l, respectively.

The adsorbent's equilibrium capacity was calculated by following Equation (2)

$$q_e= [(C_0-C_e)\times V)]/m \quad (2)$$

where q_e represents the amount of adsorbed metal ions per the adsorbent mass, C_0 is the initial concentration in mg/l, Ce the equilibrium concentration (mg/l) of 2,4-D in the solution, V the solution volume (ml), and m the adsorbent mass (g).

In addition, adsorption kinetics is the measure of the adsorption uptake concerning the time at a constant concentration and is employed to measure the diffusion of adsorbate in the surface of the nanoparticles, thus, two kinetic models of pseudo-first-order and pseudo-second-order were used. The equations of these two kinetic models are shown in Table 1. According to these equations, the parameters q_e and q_t are in the order of absorption capacity at the equilibrium time and t time, respectively. Also, the parameters of K_1 and K_2 are pseudo-first-order and pseudo-second-order kinetic equilibrium rate constant, respectively.

In this study, the extensive and conventional models of Freundlich, Langmuir, and Temkin isotherm used for adsorption data and presented in Table 2. In these equations, C_e is the equilibrium concentration of the adsorbed material (mg/l), q_e is the adsorption capacity of the adsorbent at equilibrium time (mg/g), q_m is the maximum adsorption capacity (mg/g), K_l is the constant equilibrium of Langmuir (mg/l) which is dependent on the absorption enthalpy. In the Freundlich isotherm model, K_f and $1/n_f$ is

Table 2. The values of the parameters of equilibrium isotherm models on Fe_3O_4@SiO_2-NH_2 adsorption

Isotherm model	Expression	Model parameters	R^2
Langmuir	$\frac{C_e}{q_e} = \frac{1}{K_l \times q_m} + \frac{C_e}{q_m}$	K_L = 0.781 q_m= 116.3	0.997
Freundlich	$q_e = k_f C_e^{1/n_f}$	K_f = 25.81 n_f= 3.75	0.9877
Temkin	$q_e = RT\ln(a_t C_e)/b_t$	b_t = 8.0041 a_t = 44.70	0.962

Table 3. Thermodynamic parameters of adsorption of 2,4-D toxin on Fe_3O_4@SiO_2-NH_2 adsorbent.

T (K)	$\ln K_c$	ΔG^0	ΔH^0	ΔS^0
293	2.827	-6886.36	14.1612	72.566
303	3.221	-8114		
313	3.333	-8672.7		
323	3.382	9083.3		

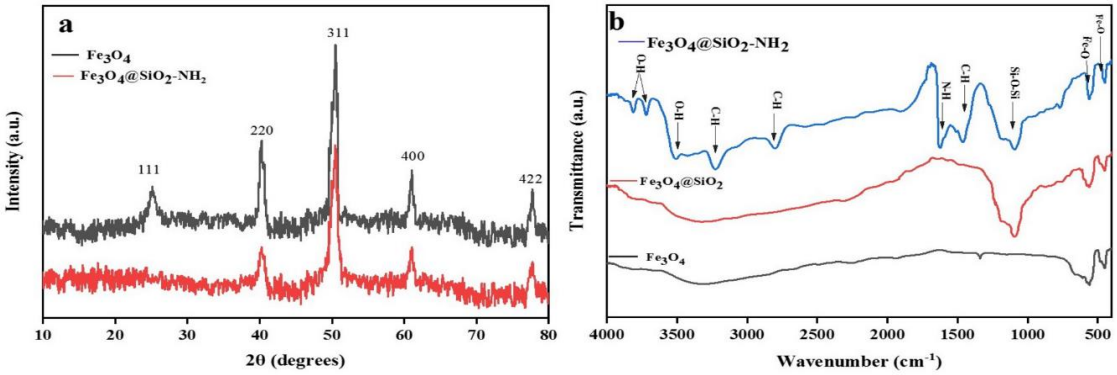

Fig. 1. a) XRD pattern and b) FT-IR Fourier Transform Infrared Spectroscopy obtained from synthesized nanoparticle samples

representative of the Freundlich and the absorption intensity, respectively. The values of the Langmuir isotherm parameters are determined by drawing the C_e/q_e diagram against C_e and for the Freundlich against $\ln C_e$. In the Temkin model, RT and b_t are the constants of this isotherm that their values can be determined by the intercept and the slope of the diagram using the q_e diagram in terms of $\ln C_e$.

Equations 3 and 4 were used to investigate the thermodynamics of the adsorption process (Table 3). In this equation, K_c is (equilibrium constant), R represents the global constant of gases (318.8 kJ/mol) and T is the absolute temperature in terms of Kelvin; the graph of $\ln K_c$ vs T^{-1} was plotted against $\ln K_c$ to determine the parameters of enthalpy (ΔH °) and entropy (ΔS °). ΔG ° is the free energy of Gibbs in terms of kJ/mol [1].

$$\ln K_c = -(\Delta H^\circ)/RT + (\Delta S^\circ)/R \quad (3)$$

$$\Delta G^\circ = -RT \ln k_c \quad (4)$$

RESULTS AND DISCUSSION

The structural properties of the materials produced

XRD analysis was used to investigate the crystallography of core-shell nanoparticles. Fig. 1a shows the XRD pattern of Fe_3O_4 magnetic nanoparticles and Fe_3O_4@SiO_2-NH_2 nanocomposite. As it can be seen in the figure of the characteristic peaks with the crystal plates, the diffraction role corresponds to the peaks of magnetic nanoparticles, which show the purity of magnetite nanoparticles and their spinel structure. Therefore, it can be concluded that the coating process has not changed the phase of Fe_3O_4 nanoparticles. Amorphous is an important and effective parameter concerning silica because crystalline silica is inactive and cannot participate

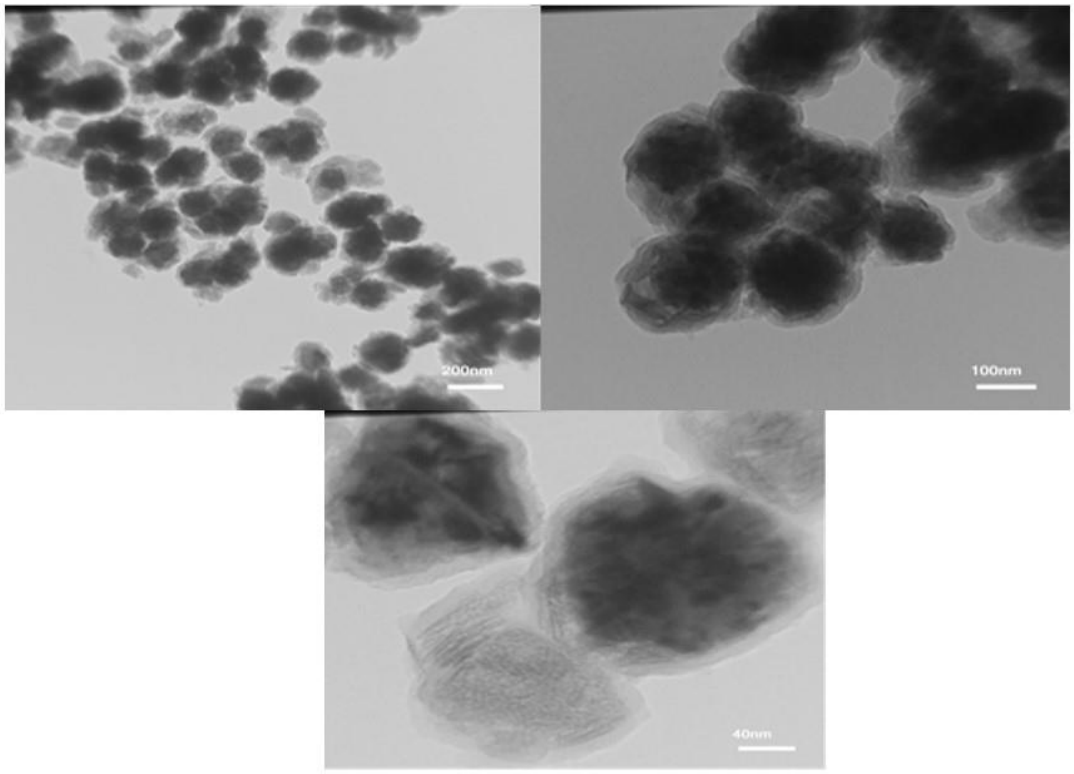

Fig. 2. TEM image of Fe_3O_4@SiO_2-NH_2 nanoparticles

in chemical reactions and its quality and efficiency are reduced. The results obtained in this section are consistent with the results obtained from previous research [18]. In the XRD pattern of Fe_3O_4 nanoparticles, 5 specific peaks are observed in the range of 25.1, 40.2, 50.4, 61.2 and 78.8 on the scale 2θ respectively, which are related to 111, 220, 311, 400 and 422, which confirms the crystal structure of the Fe_3O_4 spinel cubic. As can be seen, the peak intensity in the Fe_3O_4@SiO_2-NH_2 nanocomposite diagram has been decreased which indicates the coverage of their surface with a layer of amorphous silica and amino groups compounds [19].

Fourier Transform infrared was used to investigate the purity and bonds in the synthesized nanoparticles. As in Fig. 1b, Fe_3O_4 nanomagnetic, Fe_3O_4@SiO_2 and Fe_3O_4@SiO_2-NH_2 nanocomposites have been investigated, the infrared spectrum of magnetic nanoparticles of tensile adsorptions of Fe-O bond has appeared in the area of 447.32 and 563.96 [20]. Also, the peaks in the 3500 to 3800 area are due to the tensile vibrations of the H-O-H bond and related to the presence of water. Bond 1012.14 is related to the Si-O-Si vibration, which indicates that the silica coating has been successfully applied to the Fe_3O_4 nanoparticle [21]. Peaks 1453 to 3202 belong to the methyl tensile vibrations of Fe_3O_4@SiO_2-NH_2 composite nanoparticles group and it is the result of the formation of a silica shell on magnetic nanoparticles and the functionalization of silica shell from amino. The presence of many hydroxyl groups on the surface of nanoparticles leads to the reaction with (3-Aminopropyl) triethoxysilane and the formation of Si-O bonds in the terminal, which supports the NH functional groups in the Fe_3O_4 core nanoparticles [19].

The morphological structure and diameter of Fe_3O_4 and Fe_3O_4@SiO_2-NH_2 nanoparticles by analyzing TEM images have been shown in Fig. 2. In TEM images, it can be seen that both nanoparticles are almost spherical and have a smooth surface. The average diameter of Fe_3O_4 and Fe_3O_4@SiO_2-NH_2 is 130 nm. In TEM image of Fig. 2 of nanoparticles, a thin and relatively clear silica coating relative to whole core particles is certain. The shell thickness of the SiO_2 is important for preparing composite with the highest magnetic property for better recovery. The average diameter of nanoparticles after modification by TEOS and APTMS increased from 21.6 to 130.7 nm. This is

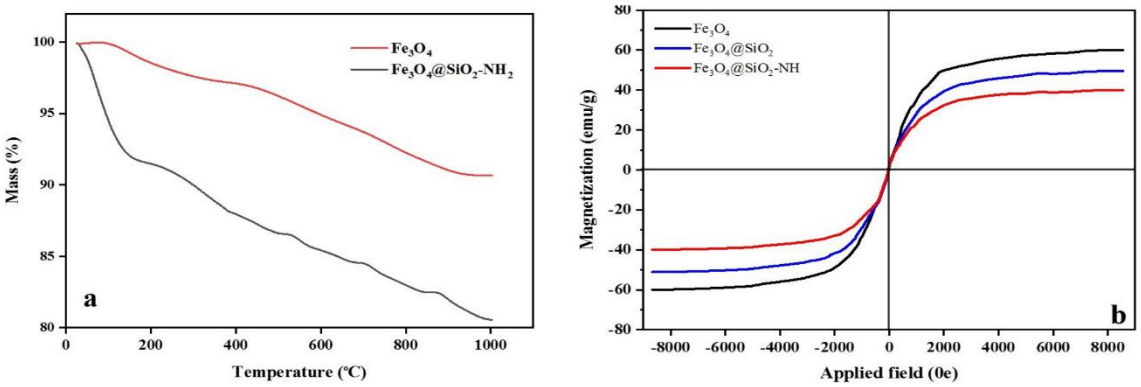

Fig. 3. a) TGA thermal analysis and b) VSM magnetic analysis of synthesized nanoparticles Fe_3O_4@SiO_2-NH_2

created by the silica shell and amine groups at the Fe_3O_4 core level. As a result, the average diameter of Fe_3O_4@SiO_2-NH_2 nanoparticles is much larger than Fe_3O_4-free nanoparticles. Therefore, nanoparticles show uniformity and satisfactory diffusion [22].

Fig. 3a shows the TGA thermal analysis curve for magnetite nanoparticles that shows the resistance of magnetic nanoparticles against heat. In general, in all TGA curve, weight loss in the approximate range of 80 to 200°C is attributed to the evaporation of water absorbed physically or chemically into the nanoparticle level. Comparison of the percentage of weight loss in the TGA curve related to Fe_3O_4@ SiO_2-NH_2 and the TGA curve related to pure Fe_3O_4 nanoparticles shows that the TGA curve related to pure Fe_3O_4 has a weight loss equal to 8%, and the weight loss of 19% related to Fe_3O_4@SiO_2-NH_2 nanoparticles which is the destruction of the amine group and the silane compounds.

To investigate the magnetic properties of the Fe_3O_4@SiO_2-NH_2 core-shell nanoparticle curve in the field, -9000 to +9000 Oe was drawn, which can be seen in Fig. 3b. The magnetic curves for Fe_3O_4, and the nanocomposite Fe_3O_4@SiO_2-NH_2, Fe_3O_4@ SiO_2 show that they have little ferromagnetic properties (due to the narrow hysteresis loop) and, as shown in the curves, the layer of Fe_3O_4 particles reduce its magnetic properties so that the saturated magnetic property for Fe_3O_4 is reduced from 60emu/g to 39 emu/g 39 for Fe_3O_4@SiO_2-NH_2 particles. This reduction is dependent on the thickness of the coated layers on the particles so that the higher the coverage, the greater the reduction in saturation magnetic property; still Fe_3O_4@SiO_2-NH_2 composite with a core-shell structure have a strong magnetic property that is strong for magnetic separation and they are very suitable for separation and recovery [1, 22].

Effects of pH, time and dose of optimal adsorption on the removal of a 2,4-D solution by Fe_3O_4@SiO_2-NH_2 nanoparticles

The effect of pH is shown in Fig. 4a. The effect of pH on 2,4-D adsorption by a change in pH (3,6,7,9,11), initial concentration of 20 mg/L of 2,4-D solution, adsorbent dose 0.2 mg/L, contact time 120 min, mixer speed 400 rpm and temperature 25°C were examined. As can be seen in the diagram, the highest adsorption rate occurred at pH= 6 and its absorption efficiency was 65.24% and the lowest adsorption rate was at pH=11 and the absorption efficiency was 34.56%. In addition, the efficiency of the removal of 2,4-D has been reduced by increasing pH. High yields at acidic pHs, especially at pH equal 6 in this study, could be due to the electrostatic force between the molecules with a negative charge of 2,4-D and the surface with the positive charge of an adsorbent. In the surface adsorption process, the pH of the solution plays an important role in the adsorption capacity and it can affect the surface load and the functional groups on the adsorbent surface. According to the results of the present study, the rate of absorption of 2,4-D in low and acidic pHs is higher than high and alkaline pH because low pH increases the percentage of protonation of NH_2 groups; and on the other hand, the rate of removal of toxin from pH has been decreased from 6 to 11 from 65.24 to 34.56%. This issue could be due to the high presence of basic ions of -OH in the solution. These ions can negate the adsorbent surface and subsequently create an electrostatic repulsive force between molecules

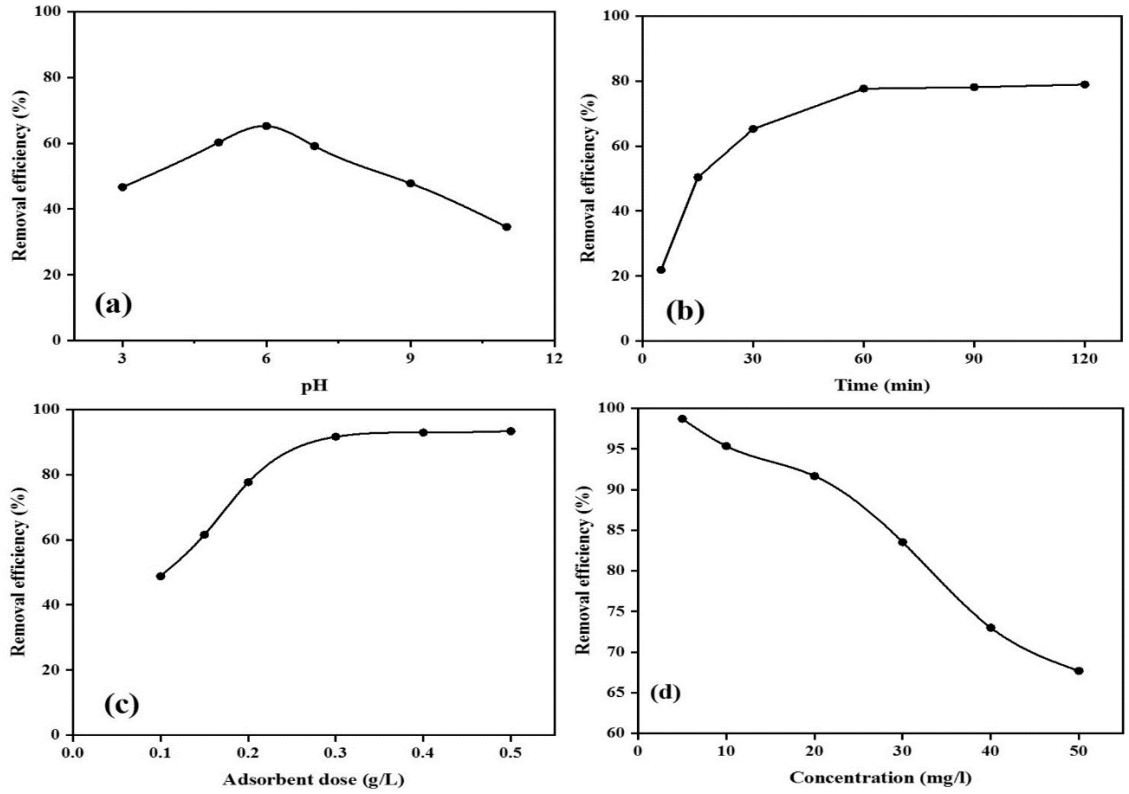

Fig. 4. a. The effect of soluble pH on adsorption efficiency b. The effect of contact time on adsorption capacity at pH = 6 c. The effect of adsorbent dose d. Different concentrations of 2,4-D on adsorption rate by $Fe_3O_4@SiO_2$-NH_2 nanoparticles

with a negative charge of 2,4-D and a surface with a negative charge of absorbent. This phenomenon causes less contribution than 2,4-D to be absorbed by the adsorbent [23]. In a study conducted by Tang et al., the optimal pH for removal of 2,4-D using Fe/OMC adsorbent was reported to be about 3 [24].

The effect of time on absorbing 2,4-D is shown in Fig. 4b. As can be seen, the absorption capacity (q_t) of the 2,4-D toxin is increased by increasing contact time from the beginning of the process to 60 min so that its value increased from 0 to 75.6% and then the amount of adsorption capacity has been almost constant. Thus, 60 min time was selected as the 2,4-D absorption equilibrium time. Examining the effect of contact time shows that the percentage of absorption is high by passing time from zero to 60 minutes and it may be adsorbent due to the presence of active and unsaturated sites on the outer surface in the first 60 minutes [25]. In Leo et al.'s study, the optimal removal time of 2,4-D by MIEX resin was considered 90 min [1].

The effect of adsorbent dose on the absorption rate is examined in five different states. Here the different concentrations of nanoparticles in values (0.1, 0.2, 0.3, 0.4 and 0.5 g/L) at pH 6, the initial concentration 20 mg/L of pollutants were investigated. The results, according to Fig. 5c, show that the absorption efficiency has been increased by increasing the adsorbent dose to the optimal value. The effect of adsorbent dose on the removal efficiency of 2,4-D is highly dependent on $Fe_3O_4@SiO_2$-NH_2 absorption rate. So that by increasing the adsorbent rate from 0.1 to 0.5 g/l, the percentage removal amount of 2,4-D increased from 48.78% to 93.36%. The increase in absorption percentage, in this case, maybe due to the presence of active sites and more surface area on the adsorbent surface, which leads to an increase in 2,4-D absorption on the surface. On the other hand, the rate of removal of 2,4-D solution has been increased by less than 2% due to the deficiency of 2,4-D molecules after a dose of 0.3 g/L. Thus, the optimal dose of adsorbent 0.3 g/L was selected.

The effect of the initial concentration of the 2,4-D solution on the adsorption rate by $Fe_3O_4@SiO_2$-

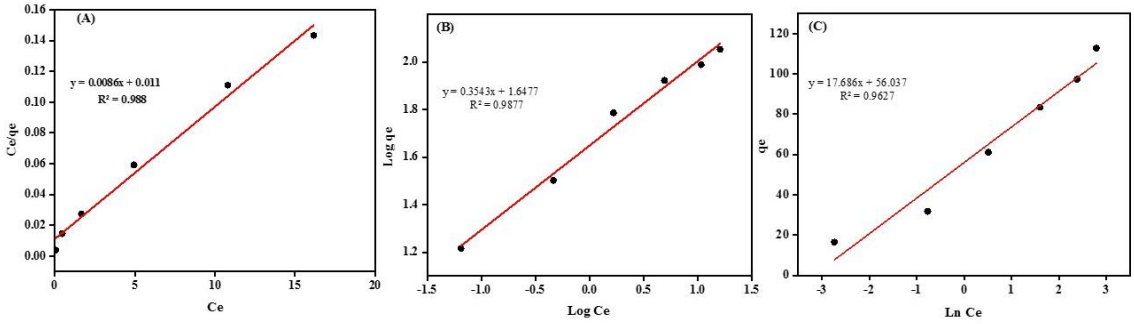

Fig. 5. A) The curve of Langmuir model, B) The curve of Freundlich model and C) The curve of Temkin model of equilibrium isotherm models of 2,4-D adsorption on Fe_3O_4@SiO_2-NH_2 adsorbent

NH nanoparticles is shown in Fig. 4d. As can be seen, with the increase in the initial concentration of 2,4-D, the decrease in adsorption was noticeable. Thus, with the increase in the initial concentration from 5 to 50mg/l, the adsorption rate decreased from 98.7 to 67.66%. Given that at a concentration of 10 mg/l, 95% of the 2,4-D solution was removed, a significant decrease in the absorption rate was observed after increasing the concentration, so the concentration of 10 mg/l was selected as the optimal concentration.

Isotherm and adsorption kinetics

In the present study, to evaluate the factors affecting the reaction speed of adsorption process of the 2,4-D contaminant on Fe_3O_4@SiO_2-NH_2 adsorbents, pseudo-first-order, and pseudo-second-order kinetic models, which have the most use in the adsorption studies, were used. The values of the kinetic parameters are shown in Table 1.

According to this table, the correlation coefficient of the two pseudo-first and second-order synthetic models is 89% and 99%, respectively. Also, according to the constant values of velocity (K_2) and adsorption capacity at equilibrium (qe), it can be said that the adsorption behavior follows the pseudo-second-order model, so the results show that the absorption of 2,4-D on Fe_3O_4@SiO_2-NH_2 adsorbent depends on the presence of active sites on the adsorbent and the adsorption process is the chemical type [26]. In the study, Sano et al. used Fe_3O_4@SiO_2-NH_2 adsorbent to remove heavy metals; The results of this study follow the pseud-second-order kinetic model and it is consistent with the present study [27]. Also, Freundlich, Longmuir, and Temkin isotherms were used to investigate the equilibrium of 2,4-D adsorption on Fe_3O_4@SiO_2-NH_2 adsorbent.

Fig. 5 shows the diagrams of the parameters related to the three models. According to the comparison of the correlation coefficients, it can be stated that the adsorption of 2,4-D on Fe_3O_4@SiO_2-NH_2 adsorbent follows the Langmuir single-layer model ($0.99<R^2$). The maximum absorption capacity of Fe_3O_4@SiO_2-NH_2 for 2,4-D is 116.3 mg/g. The Langmuir model shows that the active sites on the adsorbent surface are evenly and homogeneously distributed, and there is no interference between the adsorbed molecules of 2,4-D on the adsorbent, while the Freundlich model expresses multi-layered adsorption with uniform distribution of adsorbent material [18]. On the other hand, the value of n, if in the range of 1-10, indicates the optimal absorption of 2,4-D molecules on Fe_3O_4@SiO_2-NH_2, which is true according to the obtained values of n. In investigating the thermodynamic results according to Table 3, it was observed that the values of ΔH° and ΔS° were obtained 14.1612 kJ/mol and 72.566 kJ/mol, respectively. The positivity of these two parameters indicates the endothermic adsorption process of the 2,4-D on the nano-adsorbent and the possibility of strong bonding of 2,4-D molecule on the nanoparticle surface [28]. And as the temperature of the solution increases, the rate of adsorption of 2,4-D by Fe_3O_4@SiO_2-NH_2 nano-adsorbent increases, followed by it, the process efficiency increases [29]. In the study conducted by Siet, the values of ΔH° and ΔS° were both positive, indicating that the process of adsorption of organic contamination on the Fe_3O_4@SiO_2-NH_2 nanoparticles was endothermic [30]. Also, in the study conducted by Salman, the adsorbent values of ΔH° and ΔS° are both positively determined [4] which are consistent with the present study.

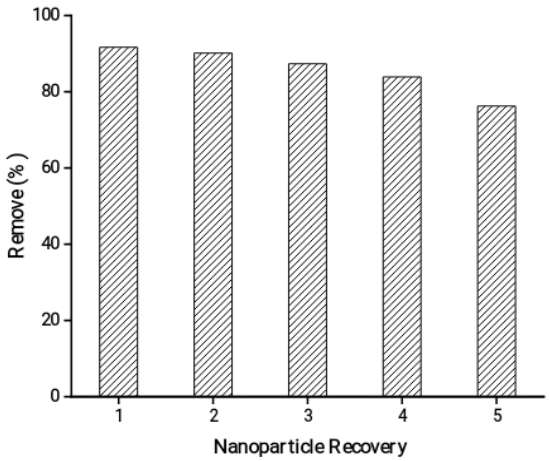

Fig. 6. Recovery of $Fe_3O_4@SiO_2$-NH_2 nanoparticles and reuse of it for absorbing 2,4-D

The reusability of $Fe_3O_4@SiO_2$-NH_2 nanoparticles

After each run, $Fe_3O_4@SiO_2$-NH_2 nanoparticles were recovered by an external magnet, washed with HCl and deionized water, and used for the next run. As Fig.6 shown, the experiment was repeated up to 5 times and no significant reduction was observed in the absorption capacity of nanoparticle. Therefore, the performance of $Fe_3O_4@SiO_2$-NH_2 nanocomposite validates its recyclability [31].

CONCLUSION

The study showed that $Fe_3O_4@SiO_2$-NH_2 nanoparticles could be a good way to remove 2,4-D contaminants from aqueous solutions due to the high efficiency, simplicity, and lack of secondary contamination in the solution. The most suitable efficacy for the removal of 2,4-D solution at pH 6, 60 minutes, and the adsorbent dose of 0.3 g/l in the initial concentration of 2,4-D solution was obtained 20 mg/l. The results showed that the adsorption of 2,4-D solution on the synthesized adsorbent followed the pseudo-second-order model of the Langmuir temperature isotherm. This action indicates that the absorption of 2,4-D contaminants on $Fe_3O_4@SiO_2$-NH_2 adsorbent is homogeneous and chemical. In addition, the study of thermodynamics revealed a direct relationship between heat and removal percentage.

ACKNOWLEDGEMENTS

This research paper was taken from a PhD thesis (ID Number: 22577/1398). The authors would like to acknowledge the valuable collaboration of faculty authorities of Natural Resources and Environmental Sciences, University of Birjand for providing necessary facilities for conduction of this study.

CONFLICT OF INTEREST

The authors declare no conflict of interest.

REFERENCE

1. Ding L, Lu X, Deng H, Zhang X. Adsorptive Removal of 2,4-Dichlorophenoxyacetic Acid (2,4-D) from Aqueous Solutions Using MIEX Resin. Industrial & Engineering Chemistry Research. 2012;51(34):11226-35.
2. Vickers NJ. Animal Communication: When I'm Calling You, Will You Answer Too? Current Biology. 2017;27(14):R713-R5.
3. MirzaHedayat B, Noorisepehr M, Dehghanifard E, Esrafili A, Norozi R. Evaluation of photocatalytic degradation of 2,4-Dinitrophenol from synthetic wastewater using Fe3O4@SiO2@TiO2/rGO magnetic nanoparticles. Journal of Molecular Liquids. 2018;264:571-8.
[4] Salman JM, Al-Saad KA. Adsorption of 2, 4-dichlorophenoxyacetic acid onto date seeds activated carbon: equilibrium, kinetic and thermodynamic studies. Int. J. Chem. Sci. 2012; 10 :677-690.
5. Ova D, Ovez B. 2,4-Dichlorophenoxyacetic acid removal from aqueous solutions via adsorption in the presence of biological contamination. Journal of Environmental Chemical Engineering. 2013;1(4):813-21.
[6] Raouf GA, Qusti SY, Ali AM, Dakhakhni TH. The mechanism of 2,4-dichlorophenoxyacetic acid neurotoxicity on rat brain tissue by using FTIR spectroscopy. Life Science Journal. 2012; 9:1686-1697.
7. Hameed BH, Salman JM, Ahmad AL. Adsorption isotherm and kinetic modeling of 2,4-D pesticide on activated carbon derived from date stones. Journal of Hazardous Materials. 2009;163(1):121-6.
8. Hoover DG, Borgonovi GE, Jones SH, Alexander M. Anomalies in mineralization of low concentrations of organic compounds in lake water and sewage. Applied and Environmental Microbiology. 1986;51(2):226-32.

9. Jung BK, Hasan Z, Jhung SH. Adsorptive removal of 2,4-dichlorophenoxyacetic acid (2,4-D) from water with a metal–organic framework. Chemical Engineering Journal. 2013;234:99-105.
10. Bazrafshan E, Kord Mostafapour F, Faridi H, Farzadkia M, Sargazi S, Sohrabi A. Removal of 2, 4-Dichlorophenoxyacetic Acid (2, 4-D) From Aqueous Environments Using Single-Walled Carbon Nanotubes. Health Scope. 2013;2(1):39-46.
11. Sayadi MH, Rashki O, Shahri E. Application of modified Spirulina platensis and Chlorella vulgaris powder on the adsorption of heavy metals from aqueous solutions. Journal of Environmental Chemical Engineering. 2019;7(3):103169.
12. Kakavandi B, Jonidi Jafari A, Rezaei Kalantary R, Nasseri S, Esrafili A, Gholizadeh A, et al. Simultaneous adsorption of lead and aniline onto magnetically recoverable carbon: optimization, modeling and mechanism. Journal of Chemical Technology & Biotechnology. 2016;91(12):3000-10.
[13] Yazdani A, Sayadi MH, Heidari A, Green biosynthesis of palladium oxide nanoparticles using dictyota indica seaweed and its application for adsorption. Journal of Water and Environmental Nanotechnology. 2018; 3:337-347.
14. Farooghi A, Sayadi MH, Rezaei MR, Allahresani A. An efficient removal of lead from aqueous solutions using FeNi 3 @SiO 2 magnetic nanocomposite. Surfaces and Interfaces. 2018;10:58-64.
15. Azarifar D, Badalkhani O, Abbasi Y. Silica-modified magnetite Fe3O4nanoparticles grafted with sulfamic acid functional groups: an efficient heterogeneous catalyst for the synthesis of 3,4-dihydropyrimidin-2(1H)-one and tetrahydrobenzo[b]pyran derivatives. Journal of Sulfur Chemistry. 2016:1-18.
[16] Tayebee R, Fattahi Abdizadeh M, Mohammadpour Amini M, Mollania N, Jalili Z, Akbarzadeh H. Fe_3O_4@SiO_2-NH_2 as an efficient nanomagnetic carrier for controlled loading and release of acyclovir. International Journal of Nano Dimension. 2017;8(4):365-372.
17. Ghorbani F, Kamari S. Core–shell magnetic nanocomposite of Fe3O4@SiO2@NH2 as an efficient and highly recyclable adsorbent of methyl red dye from aqueous environments. Environmental Technology & Innovation. 2019;14:100333.
18. Liu F, Niu F, Peng N, Su Y, Yang Y. Synthesis, characterization, and application of Fe3O4@SiO2–NH2 nanoparticles. RSC Advances. 2015;5(23):18128-36.
19. Saleh TA, Tuzen M, Sarı A. Magnetic vermiculite-modified by poly(trimesoyl chloride-melamine) as a sorbent for enhanced removal of bisphenol A. Journal of Environmental Chemical Engineering. 2019;7(6):103436.
20. Zou J, Peng Y-G, Tang Y-Y. A facile bi-phase synthesis of Fe3O4@SiO2 core–shell nanoparticles with tunable film thicknesses. RSC Advances. 2014;4(19):9693.
21. Spaltro A, Simonetti S, Laurella S, Ruiz D, Compañy AD, Juan A, et al. Adsorption of bentazone and imazapyc from water by using functionalized silica: Experimental and computational analysis. Journal of Contaminant Hydrology. 2019;227:103542.
22. Sayadi MH, Sobhani S, Shekari H. Photocatalytic degradation of azithromycin using GO@Fe3O4/ ZnO/ SnO2 nanocomposites. Journal of Cleaner Production. 2019;232:127-36.
[23] Arsiya F, Sayadi M, Sobhani S. Arsenic (III) adsorption using palladium nanoparticles from aqueous solution. Journal of Water and Environmental Nanotechnology. 2017; 2:166-173.
24. Tang L, Zhang S, Zeng G-M, Zhang Y, Yang G-D, Chen J, et al. Rapid adsorption of 2,4-dichlorophenoxyacetic acid by iron oxide nanoparticles-doped carboxylic ordered mesoporous carbon. Journal of Colloid and Interface Science. 2015;445:1-8.
25. Karimi, Javanshir, Sayadi, Arabyarmohammadi. Arsenic Removal from Mining Effluents Using Plant-Mediated, Green-Synthesized Iron Nanoparticles. Processes. 2019;7(10):759.
26. Rudzinski W, Plazinski W. On the applicability of the pseudo-second order equation to represent the kinetics of adsorption at solid/solution interfaces: a theoretical analysis based on the statistical rate theory. Adsorption. 2009;15(2):181-92.
27. Wang J, Zheng S, Shao Y, Liu J, Xu Z, Zhu D. Amino-functionalized Fe3O4@SiO2 core–shell magnetic nanomaterial as a novel adsorbent for aqueous heavy metals removal. Journal of Colloid and Interface Science. 2010;349(1):293-9.
28. Xin X, Wei Q, Yang J, Yan L, Feng R, Chen G, et al. Highly efficient removal of heavy metal ions by amine-functionalized mesoporous Fe3O4 nanoparticles. Chemical Engineering Journal. 2012;184:132-40.
29. Ayar N, Bilgin B, Atun G. Kinetics and equilibrium studies of the herbicide 2,4-dichlorophenoxyacetic acid adsorption on bituminous shale. Chemical Engineering Journal. 2008;138(1-3):239-48.
30. Si YB, Fang GD, Zhou J, Zhou DM. Reductive transformation of 2,4-dichlorophenoxyacetic acid by nanoscale and microscale Fe3O4particles. Journal of Environmental Science and Health, Part B. 2010;45(3):233-41.
31. Shekari H, Sayadi MH, Rezaei MR, Allahresani A. Synthesis of nickel ferrite/titanium oxide magnetic nanocomposite and its use to remove hexavalent chromium from aqueous solutions. Surfaces and Interfaces. 2017;8:199-205.